Electronic Supplementary Material (ESI) for Journal of Materials Chemistry A.

3D printing of self-supported solid electrolytes made of glass-derived $Li_{1.5}Al_{0.5}Ge_{1.5}P_3O_{12}$ for all-solid-state lithium-metal batteries.

A.G. Sabato[(1)], M. Nuñez[(1)], S. Anelli[(1,2)], C.D. Sierra[(1)], J.C. Rossillo[(1)], M. Torrell[(1)], A. Pesce[(3)], G. Accardo[(3)], M. Casas-Cabanas[(3,4)] , P. López-Aranguren[(3)], A. Morata[(1)], A. Tarancón[(1, 5)]

(1) Catalonia Institute for Energy Research (IREC), Department of Advanced Materials for Energy, Jardins de les Dones de Negre 1, 2nd Floor, 08930 Sant Adria de Besos, Barcelona, Spain

(2) Politecnico di Torino, Department of Applied Science and Technology (DISAT), Corso Duca degli Abruzzi 24, 10129, Turin, Italy

(3) Center for Cooperative Research on Alternative Energies (CIC energiGUNE), Basque Research and Technology Alliance (BRTA), Alava Technology Park, Albert Einstein 48, 01510 Vitoria-Gasteiz, Spain.

(4) Ikerbasque Basque Foundation for Science, 48013 Bilbao, Spain

(5) ICREA, Passeig Lluís Companys 23, 08010 Barcelona, Spain

SUPPLEMENTARY INFORMATION

DSC-TGA of printed LAGP

Differential scanning calorimetry (DSC) and thermo-gravimetric analyses (TGA) (integrated TGA/DSC 1 Star system, Mettler Toledo, US) were performed on 3D printed LAGP in the as-printed green state: cured resin + LAGP in the glassy state as-received. These analyses were carried out to tailor a suitable thermal treatment to perform the debinding of the organic components and the sinter-crystallization of the remaining ceramic electrolyte material. The sample was collected by breaking a 3D printed part and analysing a fragment of 30mg placed in an alumina crucible. As reference, an empty crucible was used. The analysis was carried out from RT to 800°C with a heating rate of 5°C/min in air.

Figure S1 shows two exothermic peaks at lower temperatures (at 212°C and 375°C) correspondent to the burning of the organic portion of the sample, these peaks indeed correspond to a strong mass loss of the sample (≈38%) coherent with the composition of the paste used for the 3D printing process. At higher T the endothermic signal associated with the glass transition temperature of the glass (T_g=497°C) was detected together with a strong crystallization exothermic peak (T_c=623°C).

The tailored thermal treatment based on these results consisted of a first slow ramp (0.2 °C/min) up to 400°C with a dwelling of 2 h, to complete burn the organic part and allow the resulting gases evacuation, followed by a step at 750°C for 12h to obtain the complete crystallization of the LAGP and promote the densification.

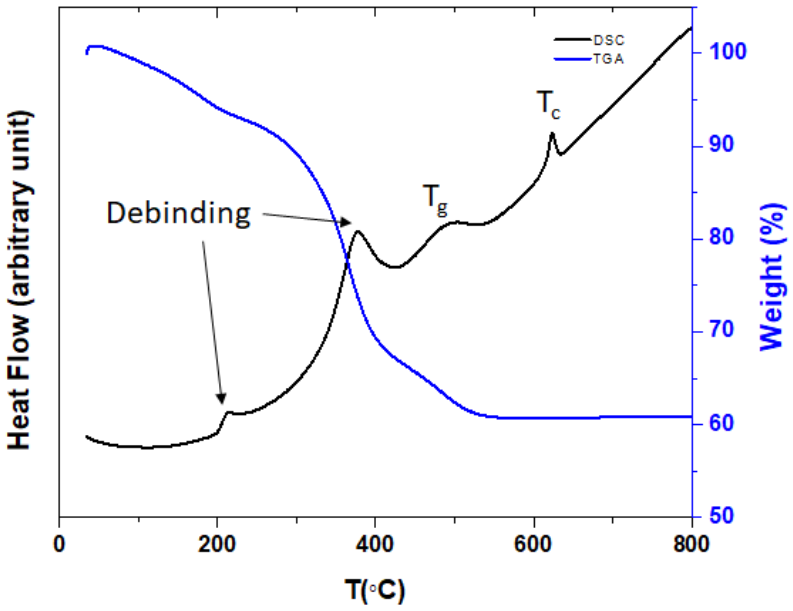

Figure S1: DSC-TGA analyses of 3D-printed LAGP in the green state (as-printed).

EIS at different temperatures

Below, the EIS spectra collected on 3D printed LAGP (both the reference membrane and the corrugated one) at different T between 25°C and 75°C are reported (Figure S2 and S3).

The EIS spectra were fitted using the equivalent circuit mentioned in the main body of the paper (Fig. 6a). An inductance L1 was introduced to fit the high frequency points ($Z'' < 0$) which become even more visible at higher T (see Figure S2 and S3), attributed to the contribution of the experimental setup. The two RC elements connected in series correspond to the contribution of the bulk (R_b and C_b) and of the grain boundaries of the material (R_{gb} and CPE_{gb}) to ionic conduction. The constant phase element (CPE_{gb}) was introduced to fit the slightly depressed semicircle corresponding to the grain boundaries. Finally, the straight line at lower frequency is due to the blocking electrodes (Au) and was fitted with a CPE element connected in series to the rest of the circuit.

For each temperature, the ASR was calculated (considering the projected area of the active membrane of each sample) and the values are shown in the main body of the present paper (Figure 6). The reference membrane was used to calculate the conductivity values of the 3D printed LAGP. This sample was chosen for its simpler shape which allowed us to calculate more precisely the conductivity for the material processed in this way. Being the conductivity an intrinsic property of the material it is legit to assume that it will be the same also for the corrugated membrane and potentially for all shapes obtained with the same process. The conductivity of 3D printed LAGP at different T is reported in Fig S4 together with the values measured on a pellet that underwent exactly the same thermal treatments and to the values collected in literature by Mariappan et al. for the same material treated at the same temperature (750°C).

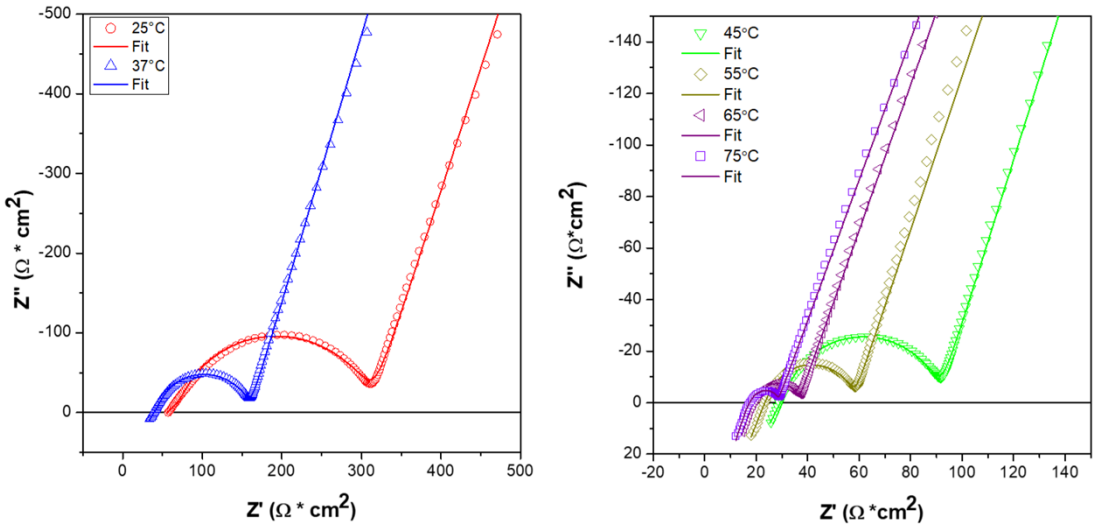

Figure S2: EIS at different temperatures of the 3D printed reference (flat) membrane.

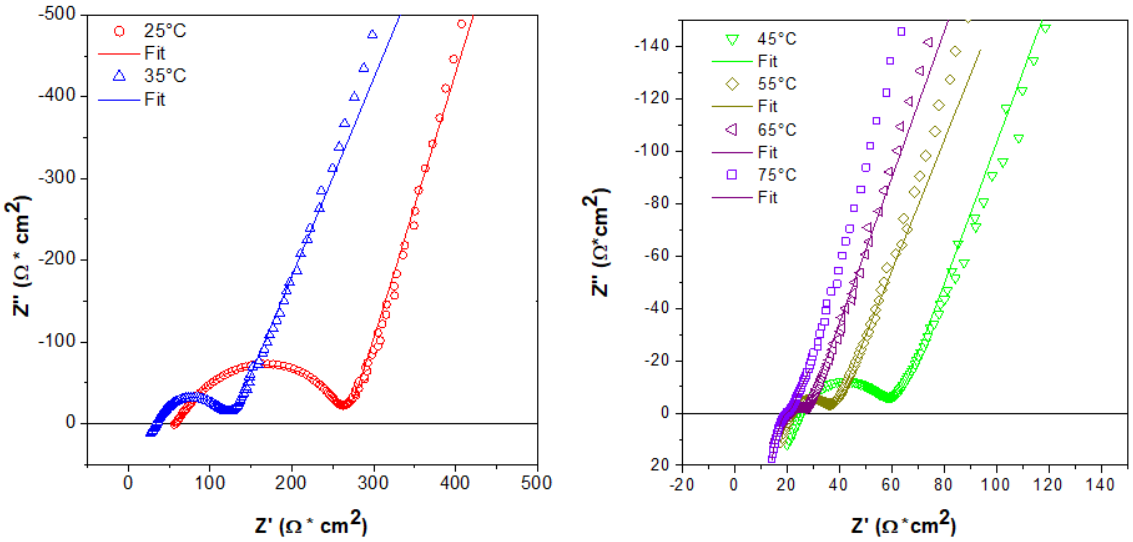

Figure S3: EIS at different temperatures of the 3D printed corrugated membrane.

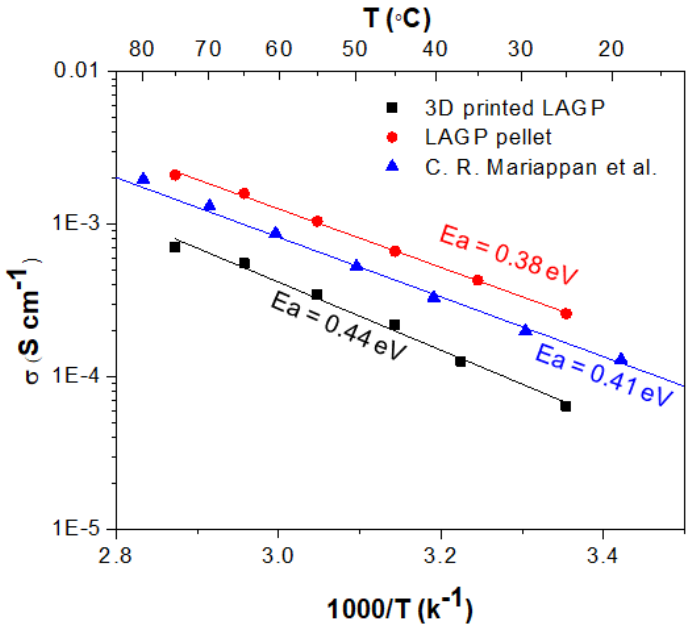

Figure S4: temperature dependence of the ionic conductivity of LAGP: 3D printed by SLA (black), produced in form of pellet (red) and reported in ref. [1] (blue).

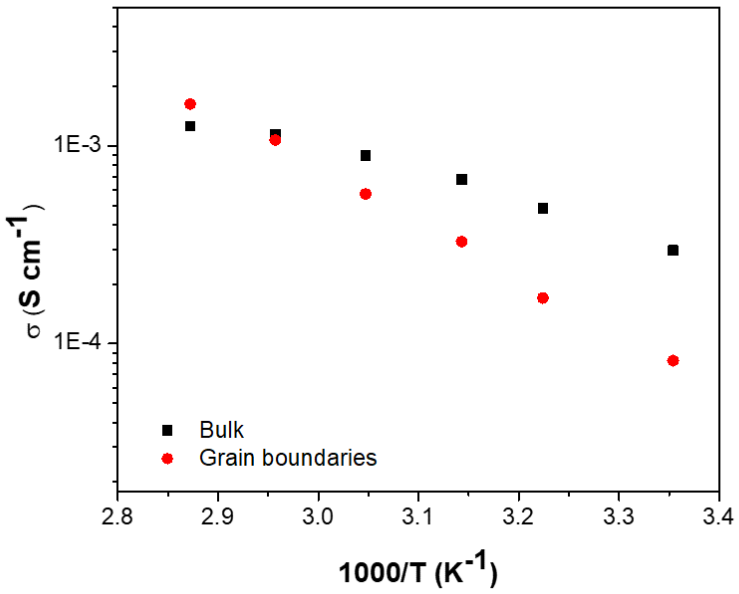

Figure S5: bulk and grain boundary ionic conductivity contribution at different T for 3D printed LAGP

Raman spectroscopy

Raman spectroscopy measurements were acquired on a Xplora Nano from Horiba Scientific. The spectrum as acquired with a 532 nm laser with 9 mW laser power and a 1800 g/mm, an acquisition time of 2 seconds and 60 accumulations. The obtained spectra (Fig. S6) only shows peaks corresponding to the LAGP phase, in agreement with the XRD presented in Fig. 5 (main body of the paper) and with other Raman measurements reported in literature [2,3]. There

are no signs of the typical D and G Carbon Raman modes, typically located at ~1350 and 1550 cm^{-1}, respectively. This measurement supports the idea of the full removal of the carbon present in the 3D-printing paste and corroborates the phase purity of the 3D ceramic piece.

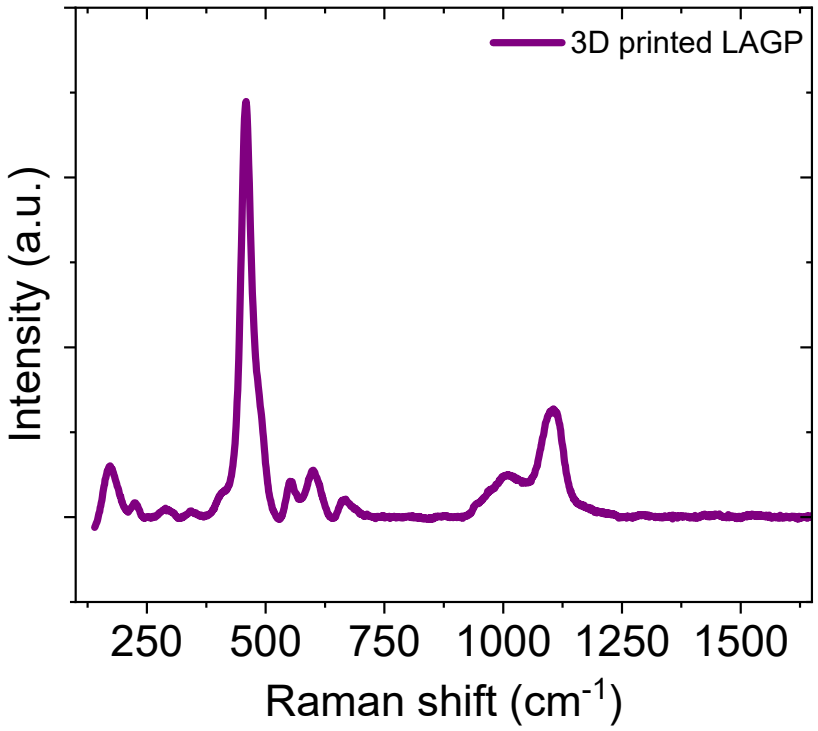

Figure S6: Raman spectra collected on 3D printed LAGP after debinding and sintering treatment.

References

[1] C. R. Mariappan, C. Yada, F. Rosciano, B. Roling, Correlation between micro-structural properties and ionic conductivity of Li1.5Al0.5Ge1.5(PO4)3 ceramics, J. Power Sources 196 (2011), 6456-6464. DOI: 10.1016/j.jpowsour.2011.03.065.

[2] A. Curcio, A.G. Sabato, M. Nuñez Eroles, J.C. Gonzalez-Rosillo, A. Morata, A. Tarancón, F. Ciucci, Ultrafast Crystallization and Sintering of Li 1.5 Al 0.5 Ge 1.5 (PO 4) 3 Glass and Its Impact on Ion Conduction, ACS Appl. Energy Mater. 5 (2022). https://doi.org/10.1021/acsaem.2c03009.

[3] S. V. Pershina, A.A. Pankratov, E.G. Vovkotrub, B.D. Antonov, Promising high-conductivity Li1.5Al0.5Ge1.5(PO4)3 solid electrolytes: the effect of crystallization temperature on the microstructure and transport properties, Ionics (Kiel). 25 (2019) 4713–4725. https://doi.org/10.1007/s11581-019-03021-5.